Research Square

Preprints are preliminary reports that have not undergone peer review.
They should not be considered conclusive, used to inform clinical practice,
or referenced by the media as validated information.

The geological history of plant mass extinction and terrestrial ecosystem collapse

Jennifer McElwain

jmcelwai@tcd.ie

Trinity College Dublin https://orcid.org/0000-0002-1729-6755

William Matthaeus

Trinity College Dublin https://orcid.org/0000-0002-0117-4059

Mónica Carvalho

University of Michigan

Surangi Punyasena

University of Illinois

Antonietta Knetge

Trinity College Dublin

David Keith

University of New South Wales https://orcid.org/0000-0002-7627-4150

Chris Mays

Natural History Museum Vienna https://orcid.org/0000-0002-5416-2289

Analysis

Keywords:

Posted Date: April 23rd, 2026

DOI: https://doi.org/10.21203/rs.3.rs-9282628/v1

License: This work is licensed under a Creative Commons Attribution 4.0 International License.
Read Full License

Additional Declarations: There is **NO** Competing Interest.

Abstract

The history of life on the planet has been punctuated by extreme biodiversity loss events on land and in the oceans, when the rates of extinction greatly exceeded background. Today, debates on whether human-driven extinction rates equate or exceed those that define past mass extinction events remain unresolved, largely because different metrics used in palaeobiology and conservation science hinder comparison. Here, we briefly review the magnitudes and abiotic drivers of past plant extinction events, examine their global climatic context compared to today and critically evaluate metrics used to define fossil plant mass extinction. We apply concepts adapted from the International Union for the Conservation of Nature (IUCN) Red List of Ecosystems to examine the fate of past terrestrial ecosystems at five faunal mass extinction events. We show that IUCN concepts can be applied to plant fossils to quantify the magnitude of extinction risk and to test between alternative hypotheses on ecosystem collapse. Our analysis suggests there is strong evidence for ecosystem collapse in the Late Devonian, mid-late Pennsylvanian, end-Permian, end-Triassic and end-Cretaceous. We show that ecosystem collapse during four of the five examined events is characterized by a transition to a novel ecosystem post-collapse rather than by an expansion of the antecedent ecospace.

Introduction

Mass extinction events in Earth history are important to study because they tell us about ecosystem disruption in the past, their environmental drivers, and the processes which shaped the re-establishment of stable communities in their aftermath. However, current definitions of mass extinction events[1,2] (Extended Table 1) do not capture the best measures of ecosystem disruption or ecological consequences and have been criticized for their imprecision[3]. Further, methods and concepts used to identify past mass extinctions are often not applicable to contemporary times and vice versa, which limits the relevance of insights gleaned from the palaeobiological record to conservation policy. Can we develop metrics of extinction (Extended Table 1) or extinction risk that are useful in drawing comparisons between the deep past and today?

In contemporary ecosystems, a species' extinction risk can be modelled as a function of the number of mature individuals within a population, the geographical extent and number of populations, and the magnitude of declines in these metrics on short timescales (< thousands of years) following International Union for the Conservation of Nature[4] protocols. Species which are categorized as most likely to go extinct on the IUCN Red List of Threatened Species—termed 'critically endangered, endangered and vulnerable'—are those with small global population sizes, narrow geographic ranges (<20,000 km^2) and/or restricted or fluctuating population numbers[5] (Extended Table 1). Based on these criteria, it is reasonable to argue that the plant fossil record likely does not provide sufficient data to retroactively construct a 'Red List' of fossil plants against which actual patterns of biodiversity loss and extinction risk could be compared. This is because the fossil record is biased against preserving species with rare occurrences or those with small geographic ranges, low overall biomass (due largely to their low abundances), and species which collectively produce fewer plant parts entering depositional

environments. Moreover, the temporal resolution of the plant fossil record is typically not of a fine enough scale to determine short-term fluctuations of past plant populations.

When examining plant mass extinctions in Earth's history, therefore, the plant fossil record is biased against detecting the extinctions of rare taxa, which are the most at risk of extinction[6]. Even when ecologically rare taxa do appear in the microfossil (e.g., spores, pollen) or macrofossil (e.g., leaves, reproductive structures) records, they often only occur once per locality or geological stage (termed 'singletons') and could represent reworking or misidentification; they are thus often treated as sampling errors and removed from palaeodiversity metrics to minimize distortions[7]. It is apparent therefore that the fossil taxa most likely represented in the geological record are those that the IUCN would categorize as 'of least concern' in relation to extinction risk. Ecological theory[8], field-based observations[9], and modelling studies[10], on which the IUCN Red List categories are based, demonstrate that extinction risks increase with ecological rarity and that extreme environmental and biotic disturbance preferentially impact taxa with low abundances. In the case of deep time, however, evidence from marine invertebrates[6] and our own analysis (Fig. 1) demonstrate that mass extinctions break the normal ecological and microevolutionary rules, as dominant species with wide geographical ranges and belonging to species-rich clades do not guarantee survivorship during mass extinction events (Fig. 1).

Here, we suggest that metrics of past mass extinction events that are based solely on the loss of taxonomic richness or an elevation of extinction rate beyond background (Extended Table 1) may be inadequate, because they do not consider differences in ecological roles of taxa that go extinct. They, therefore, provide limited insights into ecosystem-level consequences of mass extinction events. Further, they have a very low probability of capturing the ecologically rare and uncommon taxa of past ecosystems due to taphonomic biases and poor taxonomic resolution. For instance, many species of fossil plants cannot be recognized due to insufficient character preservation, implying that we are missing high levels of cryptic extinction (Extended Table 2). To compare deep-time records with contemporary extinction metrics, an alternative metric is therefore required: one that works with the strengths of the fossil record by focusing on the fossil species with high relative abundances indicative of commonness and ecological dominance.

According to Grime's[11] mass ratio theory, the main functioning of terrestrial ecosystems in terms of net primary productivity is predominantly controlled by dominant taxa. Further, experiments and observations in contemporary ecosystems show that perturbations that drive losses in the relative abundances of common taxa can negatively impact the resilience and functioning (e.g., net primary productivity) of plant communities by a greater, or at least similar, magnitude as rare species losses[12,13], but can also drive extinction of rare taxa[14,15]. Since plants comprise >85% of all biomass on Earth[16] and many terrestrial biomes are dominated by very small numbers of taxa[17], we predict that major land ecosystem changes and multiple lineage extinctions can occur with only modest losses in plant diversity. As information on abundance becomes increasingly available from plant macro- and microfossil datasets, changes in fossil group abundances can be an important variable in measuring

plant responses to major environmental perturbations of the past, particularly their application to understanding terrestrial ecosystem change.

In contemporary ecology, it is widely documented that declines in the abundance of dominant species within an ecosystem negatively impacts whole ecosystem function[12,13]. Interestingly, 'declines in abundance' metrics are currently used as part of the IUCN's Red List of Ecosystems (Criterion D) to evaluate the conservation status and assess extinction (or 'collapse') risk of whole ecosystems rather than individual species. An ecosystem is defined as collapsed—the worst case scenario for ecosystem conservation—"when it is virtually certain that its defining biotic or abiotic features are lost from all occurrences, and the characteristic native biota are no longer sustained. Collapse may occur when most of the diagnostic components of the characteristic native biota are lost from the system, or when functional components (biota that perform key roles in ecosystem organisation) are greatly reduced in abundance and lose the ability to recruit" (p. 7)[18]. Dominant plants are keystones of terrestrial ecosystems. We therefore propose a broader conceptualization of mass extinction events that considers both evolutionary and ecological metrics of floristic change (Extended Table 1).

Building on previous work[19–21], and the concept of ecosystem collapse in the IUCN Red List for Ecosystems criteria[18,22], we propose novel criteria for diagnosing ecosystem collapse in palaeoenvironments and over geological time frames. These criteria provide a method of assessing ecological disruption that is missing from conventional mass extinction metrics and provides a means of cross-comparison between deep-time and contemporary datasets for many different evolutionary groups although we restrict our application here to terrestrial plants.

We propose that an ecosystem collapse in the plant fossil record (Extended Table 1) can be evidenced by substantial and permanent reduction in the relative abundances of the dominant plant taxa (fossil-species or -genera) and/or change in the occupied ecospace (defined as the multidimensional compositional space of a fossil plant assemblage using multivariate statistical analyses) of the palaeoecosystem within a geologically short timeframe (~100kY), based on a time-series of macro- and/or microfossil assemblage records (Extended Table 1).

To meet the IUCN's outcome of ecosystem collapse, the scale of reduction in relative abundance of the dominants or shift in ecospace should exceed the usual background variability in ecosystem composition, function, and/or structure that results from stochastic or cyclical processes influencing vegetation dynamics, following Keith et al.[22] (Extended Table 1). Furthermore, the scale of ecosystem change should be sufficient to meet one or more of the IUCN criteria for 'ecosystem collapse' (listed in Extended Table 1). The advantage of applying this concept to the fossil plant record of past mass extinctions is that unlike species, ecosystems do not disappear per se (as in species extinction), but are replaced by novel or nearby ecosystem types[22]. We therefore have a much higher probability of identifying and quantifying an ecosystem collapse in the geological past than capturing the last occurrences of species (e.g., the Signor-Lipps effect[23]). To accurately measure changes in ecosystem function and composition, absolute abundances estimates should be applied where possible (e.g., [24–

[27]), since these are divorced from the issues inherent to relative abundance data, such as compositional effects[28].

Considering the complementary definitions of mass extinction and ecosystem collapse, we review recent advances in the literature and critically appraise five biotic extinction intervals in Earth history: the Late Devonian extinction interval: the Mid-Late Pennsylvanian plant extinction event and the end-Permian, end-Triassic and end-Cretaceous extinction events. We ask whether the floristic compositions of these extinction intervals are characterized by diversity loss, major ecological change, or both, and what were the associated functional, and/or structural changes? Specifically, we: (i) re-analyse the floristic record of mass extinction of Cascales-Miñana & Cleal[2] using updated chronostratigraphy and alternative statistical definitions of mass extinction (Extended Table 1); (ii) use multivariate analyses on published microfossil and macrofossil abundance datasets spanning four of the five extinction intervals to determine if there is evidence for ecosystem collapse (Extended Table 1), and (iii) highlight recent advances in understanding of plant responses to extinction events and avenues for future study.

Late Devonian mass extinctions

Two events – the end-Frasnian 'Kellwasser Event'[29] and the end-Devonian 'Hangenberg Event'[30] – collectively make up a protracted, multi-stage interval of Late Devonian mass extinctions between 372 and 358 million years ago. We have therefore grouped both events here under the umbrella of the 'Late Devonian Mass Extinctions' (LDME)[31]. Based on marine invertebrate biodiversity losses, the end-Frasnian was originally included as one of the 'Big 5' faunal mass extinction events[1], but extinction rates of the end-Devonian event may have reached similar magnitudes[30]. Faunal mass extinctions in the Late Devonian occurred against a backdrop of ~20 million years of climate state changes from 'transitional' to 'coolhouse' to 'coldhouse'[32] (Fig. 2). There is also widespread evidence for multi-phased extinction pulses of marine invertebrate fauna and climatic/environmental perturbations, including oceanic anoxia[33], 100-metre-scale sea level fluctuations[34], and prominent carbon sequestration that would have significantly altered atmospheric CO_2 concentrations[35].

Understanding of the floral dynamics during the Late Devonian comes mainly from fossil pollen and spore records supplemented at intervals by localities with exceptionally well-preserved macrofossils. These assemblages suggest biogeographically cosmopolitan flora across the northern Gondwana and Laurentian palaeocontinents during the Frasnian (382–372 Ma) composed of massive, canopy-forming progymnosperms (e.g., *Archaeopteris*, *Geminospora*) and cladoxylopsids (e.g., *Cladoxylon*), ground-covering Zosterophyllopsida (e.g., *Sawdonia*), lycopsids (e.g., *Cyclostigma*, *Lagenicula*), and fern-like plants (e.g., *Diducites*, *Rhacophyton*)[36–38]. *Archaeopteris* was widespread in coastal areas fringing the Paleotethys Ocean (North America, Ireland, Belgium, China, Iran and Morocco; Fig. 1) for much of the Late Devonian, but disappeared globally during the end-Devonian[39]. These spore-bearing trees measured ~30m in height with stem diameters at chest height of over 32 cm[40] and were likely the keystone taxon of Late Devonian terrestrial ecosystems as the largest and most ecological dominant element within

Late Devonian forests[41,42] (Fig. 1). If we apply the IUCN Red List of Ecosystems criterion D (see table 5 of [22], Extended Table 3) to assess the extinction severity of the LDME, the extinction of *Archaeopteris* would constitute an ecosystem collapse. *Archaeopteris* was the defining taxon of these early gallery forest ecosystems, and despite having many traits suggestive of a stress tolerant ecology (such as branch shedding, thick bark, adventitious roots, and vegetative propagation[41]), this once globally-distributed genus did not persist as an ecosystem dominant or subdominant following the Hangenberg Event[36,43].

Many additional species of spore-producing plants went extinct near or at the end of the Famennian Age (latest Devonian, c, 359 Ma)[44]. These include a globally well-distributed, coastal near-swamp and likely homosporous plant group of unknown affinity that produced the spore-taxon *Retispora lepidophyta* (see reviews[44–46]). Prior to their extinction, *R. lepidophyta* spores show a strong pattern of size reduction throughout the Famennian[39] and an increased abundance of the developmentally malformed '*tener*' variety. This '*tener* event' may be contemporaneous or immediately precede the Hangenberg marine extinction event[45]. *Vallatisporites*, an isoetalean spore common in the Famennian, also underwent severe population decline from an extensive range of global localities[37,47]. In East Greenland, an interval of spore wall darkening and malformations occur in zygopterid ferns (*Grandispora cornuta*[48]) and in others of uncertain botanical affinity (*Verrucosisporites nitidus*) interpreted as genetic mutations caused by high UV-B radiation[46]. Greenland fossil localities exhibit a loss of woody taxa, with declining abundances and size classes of fossil woods[46], the latter perhaps suggesting decreasing tree height based on palaeo-functional trait metrics[49].

Although some agree that enhanced UV-B radiation may have been caused by depletion of the ozone layer at the time (Extended Table 3), the proximal driver of extinctions and spore mutations remains strongly contested, with supernovae[50], large igneous province volcanism[51], and climate-driven chlorine free-radical emissions[46] all proposed. Biotic stress due to climatic cooling and enhanced aridity have also been invoked for the *tener* event[45]. Major, short-lived climatic fluctuations likely triggered, in part, by one or more large igneous provinces[51] are evident during these biotic crises (see [52]), but the impacts of these changes on land plants remain unsettled.

What was the nature of the vegetation in the aftermath of the Late Devonian? In Ireland, the spore taxon *Verrucosisporites nitidus* dominates earliest Carboniferous (Tournaisian Stage) sediments. The parent plant affinities are unknown, although a link to Zygopteridales ferns has been suggested[37] as well as other ferns and lycophytes[48]. Zygopterids had drought- and disturbance-tolerant traits, including fleshy water storing rhizomes, and exhibit evidence for dormancy and arrested growth and precocious spore output with the potential to retain spores within the sporangia (endospory)[53].

Following the LDME, zygopterids contributed to the ground-cover floras and attained an ecologically dominant to co-dominant role[54] with lycophytes, true ferns and sphenopsids[55]. Early Carboniferous

forests re-developed canopy structures[38] after the global extinction of *Archaeopteris,* but remained compositionally distinct from their Late Devonian counterparts[43,56,57]. Unfortunately, no suitable fossil abundance datasets are available to examine the quantitative changes in ecospace before and after the Late Devonian mass extinction interval, but *Archaeopteris* relatives (progymnosperms), small trees (e.g., *Sanfordiacaulis*[38]) and woody seed plant groups were all present in a forest structure hypothesized as more structurally complex than those of the Late Devonian[43,56].

Significant advances have thus been made in documenting LDME timing (e.g., geochronology[58,59], floras[44,45,52]), scale of local and regional ecological change and in documenting extinction rate and magnitude at global scale[2,36,43,60]. Was there a plant mass extinction in the Late Devonian? The answer depends on how mass extinction is defined. The answer is 'no' when mass extinctions are defined by an elevation of plant family extinction rate above background[2] (Fig. 3) and when using loss of diversity metrics, since the recovery floras have high diversity[61,62] (Extended Tables 2, 3, Fig. 2). It is 'yes' when mass extinction is defined based on an elevation of generic level extinction rates[60] or on high-resolution local ecological turnover and extreme abiotic change[52]. We conclude, based on the definition of ecosystem collapse presented in this work (Extended Tables 1, 2, Fig. 4A), that there is sufficient evidence for ecosystem collapse during the Hangenberg Event (Extended Table 3), represented by substantial loss in the relative abundance of *Archaeopteris*, a dominant taxon with a wide geographic range (Fig. 1E, Extended Table 3).

Mid-Late Pennsylvanian boundary

The Mid-Late Pennsylvanian Boundary (MLPB), dated to 306 Ma, occurred within a coolhouse climate state[32,63] characterized by glacial-interglacial phases coupled with atmospheric greenhouse gas and sea-level change on 400,000 year cycles[32]. That time is analogous to our current climate state (Fig. 2) and arguably of high relevance for modern and future ecosystem changes. The MLPB is not identified as a marine invertebrate mass extinction event. However, we include it here because global analyses of fossil plant families indicate overturn in MLPB terrestrial floras[64], characterized by seed plants replacing spore-producing plants, and ultimately, water-stress-tolerant conifers emerging as global dominants[65].

Preceding the MLPB, Carboniferous (359–299 Ma) tropics were dominated by lepidodendralean forests (i.e., the 'Carboniferous coal swamps') during wet periods of glacial-interglacial cycles[66]. This 18-million-year-long equilibrium tropical biome ended abruptly with the regional extinction of tree lycopsids (e.g., *Lepidodendron* macrofossils and *Lycospora* microfossils) at the MLBP[67] (Fig. 1). The extinctions are thought to have been geologically synchronous across the Illinois and Donets basins in North America and Ukraine[64]. Given the functional role of spore-producing trees in these ecosystems, our assessment using the IUCN Red List of Ecosystems criteria is that the MLBP is an unequivocal case of ecosystem collapse (Extended Table 3; Fig. 4), strongly supporting decades of seminal work[64,68,69]. Lycopsid trees did not go globally extinct as they persisted in China into the Permian[70] but they were extirpated from the

majority of their global range (Fig. 1). In North American deposits, 67% of species were extirpated from peat-forming mires and more than half of clastic swamp species went extinct[69]. Despite this, family-level extinctions did not exceed background rates[2] (Fig. 3). Hence, the MLPB fails to qualify as a mass extinction under some definitions (Extended Table 1). Of all events examined herein, the decoupling of extinction rates (Fig. 3) and relative abundance changes (Fig. 4) during the MLPB provides the clearest demonstration of how mass extinction and ecosystem collapse may be expressed differently for Kingdom Plantae, and how these concepts should be investigated in parallel.

In European palaeofloras, *Lycospora*-producing plants persisted marginally until the latest Carboniferous, with strong reductions in lycopsid relative abundances occurring first in upland interior areas and lastly in lowland coastal areas[71]. Proposed causes of the lycopsid decline include population fragmentation[66], increased moisture seasonality[72] coupled with water-sensitive lycopsid physiology[73], sudden global warming[63,74], and uplift-induced drainage[75]. A potential, though unconfirmed, trophic consequence is noted in the tetrapod fossil record (i.e., the 'Kasimovian bottleneck')[76].

The MLPB ecosystem collapse changed the structure and functioning of post-MLPB forests. These were dominated by pteridosperms ('seed ferns') and more water stress-tolerant marattialean tree ferns, and then by early-diverging conifers[77]. Krings et al.[78] suggested that the canopy may have become more closed with tree fern dominance, which in turn allowed vines to thrive, but canopy-closure proxies (e.g., [79]) have not yet been applied to test this hypothesis. Palaeoecosystem modelling demonstrates that the MLPB altered plant-driven water cycling by a sufficient magnitude to contribute to Permian climatic aridification[80]. Similarly, the MLPB ecosystem collapse likely impacted the carbon cycle, which became diminished post-MLPB, and the close phasing relationship of the pre-MLPB climate and carbon cycle become abruptly anti-phased following the MLPB[81]. Community instability occurred in North American coal swamp localities after lycopsids extirpation and before fern dominance[67]. Interestingly, herbaceous isoetalean lycopsids (*Chaloneria*) proliferated briefly[67], perhaps analogous to lycopsid proliferation following the end-Permian event (see below). This time of ecological instability in the immediate aftermath of an ecosystem collapse is echoed in the other extinction events reviewed here.

End-Permian extinction event

The greatest diversity losses in Earth's history occurred at the end of the Paleozoic Era, during the end-Permian extinction event (EPE), both in the oceans[1,82] and on the continents[2]. Land biotas suffered a wave of extinctions at c. 252.3–252.1 Ma[83,84], followed by a second wave[85] that may have been concurrent with the main pulse (or pulses) of marine extinctions close to the Permian-Triassic Boundary (251.9 Ma)[86,87]. The EPE is characterized by the most extreme climate-state changes of all those discussed in this review, transitioning from coolhouse to coldhouse and then to hothouse[32]. Climatologically, the EPE therefore represents climatic change beyond all IPCC future climate scenarios, but may presage longer-term forecasts[88].

The timing and intensity of floristic changes differed by latitude. Terrestrial ecosystems at higher latitudes tended to collapse slightly earlier than those in tropical regions[84,89], while polar floras may have had a greater survivorship rate[90]. Additionally, the pace and nature of recovery varied significantly across the globe and appeared to be influenced by latitude[91,92].

The ultimate driver of the EPE was the Siberian Traps Large Igneous Province (STLIP)[93]. The intrusion of magma into the Siberian continental lithosphere led to massive greenhouse gas emissions[94]. This caused global warming of at least several degrees centigrade[95], with higher latitudes experiencing greatest warming[96]. Moreover, major changes in precipitation regimes led to regional aridification[97,98], or at least intermittent drying and/or seasonality in previously everwet environments[83,96], while promoting wildfires[99]. Precipitation-related changes likely played an even larger role than temperature in the collapse of wetland ecosystems, but this remains to be tested. Aerosols like sulfur dioxide caused temporary but severe cooling[100], and emissions of ozone-depleting compounds enhanced UV-B ionizing radiation[101,102], at least on a regional scale[103]. Metal phytotoxicants like nickel and mercury are elevated in sediments of this age, some of which have been directly linked to STLIP magmatism[104,105], and could have enhanced plant physiological stress and retarded their development. While a consensus has converged on the STLIP as the ultimate cause of EPE land ecosystem collapse, the debate now centres on the relative roles of the proximate causes (or 'kill mechanisms'), including whether some contributed at all.

Some have argued that floral communities were not severely impacted during the EPE[106,107] or did not suffer major diversity reductions[108] (Extended Table 2). However, the global fossil record of terrestrial floras reveals a greater biodiversity loss during this event than for any other biotic crisis in Earth's history on both regional (up to 95% species-level extinctions)[85] and global (c. 60% genus-level extinctions)[109] scales. While it is clear that many plant families and orders were resilient to extinction during the EPE compared to Permian animals[19,108], terrestrial floras experienced major, long-term—or in some cases permanent—ecological and physiological changes. These included sustained drops in productivity[110,111], the selective losses of keystone wetland taxa[85,112], and major changes in dominant functional traits, life history strategies[113] and biogeographic distributions[114].

During the EPE, there was a global extirpation of peatlands and the extinction of the plants that comprise them, reflected in the rock record by the onset of a 'coal gap'[115] that lasted for >7 million years[92]. The pre-EPE Permian wetlands of Gondwana and Cathaysia were dominated by peat-forming, broadleaved and typically entire-margined glossopterids[116,117] and gigantopterids[118], respectively. Both groups went extinct at the end-Permian event[117,119,120] (Fig 1). Applying the IUCN Red List for Ecosystems to categorize the severity of EPE ecosystem change, the extinction of the glossopterid- and gigantopterid-dominated floras can be interpreted as global, (near-) synchronous wetland ecosystem collapses (Fig. 1, Extended Table 3). This is supported by the distinct areas of pre- and post-EPE assemblages in ordination ecospace[110] (Fig. 4). In some regions, the absence of coal was despite the presence of local

depositional conditions that would otherwise promote their formation[121] and plant groups that would later form the bulk of Triassic coal measures[120]. This indicates that global environmental conditions—including several major climatic fluctuations following the EPE[92,122]—hindered the recovery of wetland ecosystems until c. 244 Ma (early Middle Triassic)[115].

For millions of years following the EPE, multiple surviving plant groups waxed and waned in abundance, including herbaceous lycophytes and small-leaved conifers and/or seed ferns in Gondwana[92,123], Euramerica/Angara[124,125] and Cathaysia[112]. Perhaps the most characteristic components of these Early Triassic floras were the pleuromeian lycophytes, which underwent rapid increase in spore abundance (e.g., *Aratrisporites*, *Densoisporites*)[124,126]. These were slow-growing, stress-tolerant plants lacking wood, and were emblematic of the low-productivity and low-diversity vegetation of the earliest post-EPE interval[113]. Their rise to dominance was asynchronous across the world, first occurring immediately after the EPE at low latitudes[127], before spreading to the poles during their global peak c. 2 million years after the EPE[92]. By 248.5 Ma, the tree-free, spore plant-rich episode of pleuromeian dominance had largely ended when various seed plant groups re-emerged as ecologically dominant across most landscapes. Importantly, the newly dominant taxa—conifers, ginkgoes or umkomasialean or peltaspermalean seed ferns[114,123]—went on to characterize land ecosystems for most of the Mesozoic, but are distinct from those that dominated most Paleozoic ecosystems. The EPE, therefore, highlights an important, recurrent feature of ecosystem 'recovery': Pre- and post-collapse ecosystems may eventually be structurally similar, but the primary constituents following major collapse events tend to arise from entirely different groups.

End-Triassic extinction event

The end-Triassic was a time of elevated plant extinction rate compared to background, according to our re-analysis of family-level occurrence data (Fig. 3)[2]. However, only one plant order—the Peltaspermales—went globally extinct, or 'near extinct' as it may have survived in rare occurrences into the Jurassic[128]. Ginkgoales, which are considered a close relative of Peltaspermales[129], survived the end-Triassic mass extinction, along with all other known plant orders. Peak plant extinction rates may have occurred in the earliest Jurassic (Hettangian Age), yet this pattern might be attributed to an artefact of high preservation potential rather than a true biotic extinction event[128]. Given the complexity and apparent contradictory signals, as with all the marine mass extinction boundaries, we are therefore left with the question: was there a floral mass extinction at the end of the Triassic Period?

Early work documenting >85% extinction of fossil plant species across vast sedimentary basins in East Greenland[130], Sweden[131] and the Newark Supergroup in North America[132] suggested a plant mass extinction, as defined by Jablonski[133] (Extended Table 1). Contrary arguments invoke taphonomic and sedimentary factors or issues of scale and natural variability (Extended Table 2) to account for the apparent high number of plant species extinctions. These studies stimulated further investigation using palaeoecological approaches with an aim of determining the ecological ranks of 'losers' and 'survivors'

in pre- and post-event landscapes, respectively[24,134–137]. Two exceptionally well-preserved and census-collected localities of the Jameson Land Basin of East Greenland indicate that over one third to one half of all recorded fossil plant genera went regionally extinct[24,25,134], including the Triassic ecological seed fern *Lepidopteris*, which had a wide biogeographic distribution (Fig 1). Further, these studies showed significant plant compositional shifts with evidence for a loss of the identity of the Triassic forest flora and its replacement by compositionally distinct and more homogenous forested ecosystems in the Early Jurassic[24,25,134]. When plotted in ecospace using NMDS, these compositional shifts meet the IUCN criteria of collapse of the regional Triassic forest ecosystem (Fig. 4).

The pre- and post-ETE floras are functionally distinct, which provide further evidence for an ecosystem collapse (Extended Table 3). Post-ETE species have reduced evapotranspiration rates[138] and are adapted to higher fire intensity[139]. They occupy ecosystems which are dominated by species with an ecological tolerator strategy based on their leaf functional traits[140]—likely in response to higher fire intensity and reduced evapotranspiration—providing further evidence for an ecosystem collapse. An increased abundance of aberrant/malformed spores[141–143] suggests environmental teratogens in the end-Triassic associated with extensive flood basalt volcanism in the Central Atlantic Magmatic Province (CAMP). Biotic responses to a changed abiotic environment in the end-Triassic interval lends further weight to the idea of an ecosystem collapse (Extended Table 3).

A complete turnover in the fern flora is observed in the Sichuan Basin, China, in both palynofloras and macrofloras[144,145]. Ecological dominance of Dipteridaceae/Matoniaceae ferns (62%) in the latest Triassic diminishes to 13% in the early Jurassic, while Cyatheaceae/Dicksoniaceae show an increase in their relative abundances from 21% (Rhaetian Stage) to 73% (Hettangian Stage)[145]. Based on IUCN criteria, these shifts collectively are indicative of an ecosystem collapse (Extended Tables 1, 3). Notably, the total ‘fern’ relative abundance (Dipteridaceae, Matoniaceae, Cyatheaceae, Dicksoniaceae) remains relatively unchanged across the Late Triassic and Early Jurassic (from 62 to 73%). This illustrates that presence/absence analysis at higher taxonomic ranks (e.g., ‘ferns’[128]) can mask the true underlying ecological and evolutionary patterns of mass extinction (Extended Table 2).

Fossil assemblages in the Danish, German and Austrian basins reflect hardwood gymnosperm forests of conifers (particularly Cheirolepidiaceae) and seed ferns during the latest Triassic. These were replaced by a spore-producing vegetation with dominant ferns, lycopsids and liverworts[135,136]. At St. Audries Bay (UK), abundances of Cheirolepidiaceae pollen, represented primarily by the distinctive, globally distributed taxon *Classopollis*, declined from >90% to <10%[135]. We cannot review every global flora in this short paper, however a clear pattern is emerging. The end-Triassic extinction event is characterized by reduced relative abundances of the keystone taxa or ecological dominants in every locality across the globe which has been studied at a taxonomic resolution of species, genus and family (see example taxon *Lepidopteris*, Fig. 1). The identity of the taxon undergoing loss in relative abundance is highly varied and locality-specific, yet many of the ‘losers’ of the end-Triassic had been the ecological dominants. Contemporary conservation science works on the assumption that extinction risk for plants

is likely to be less severe for species which are ecologically dominant and/or have a widespread geographic distribution[146]. IUCN redlisting of species therefore ranks those with generally narrow distributions, rapid declines and low abundances as being at high risk of extinction[146]. The end-Triassic extinction event must have been severe as dominant taxa with wide geographical distributions became rarer or experienced range constriction (Fig. 1) and perhaps contrary to expectations, some previously rare elements in the flora were recruited in the new ecosystems of the Jurassic[24]. A long episode of tree-poor and fern-rich ecosystems separate the typical end-Triassic forests and their Early Jurassic post-extinction counterparts[25]. However, unlike the protracted multi-million year ecosystem recovery after the end-Permian extinction event, new forested ecosystems were re-established within hundreds of thousands of years[25,147].

End-Cretaceous extinction event

The end-Cretaceous mass extinction event was caused by a meteorite impact[148] that struck Earth 66.02 Ma[149] and formed the Chicxulub crater on the Yucatán Peninsula, Mexico. This event is distinct from all others discussed here in that it was a geologically instantaneous event, and both biotic and abiotic responses have been documented in exquisite spatiotemporal detail. This event occurred at a time of magmatically induced warming from the Deccan Large Igneous Province[150]. Aside from the short-lived 'impact winter' that immediately followed asteroid impact (see below), global climates heated from a 'transitional' (22 to 25°C) state (Maastrichtian Age) to hothouse (28 to 36°C) conditions (Danian Age)[32], far outside Earth's current and near future climate state (Fig. 2).

The energy of the asteroid produced a ~50km diameter crater and a >130m diameter ring of melt rock on impact[148,151]. Globally, the time of the impact is marked by an event horizon of soot, charcoal, shocked quartz, rare earth anomalies and tsunami deposits[151,152], enabling cross-comparisons of vegetation responses between continents and hemispheres. The force of the impact ejected 12,000 GT[152] of solid sediments (fine, micron scale calcium carbonate dust, shocked quartz) into the global atmosphere, which rained out over the course of weeks. This estimated mass of solid particulates is 4.8 times that of the mass of the asteroid[152]. Large quantities of sulphur- and iron-rich nanoparticles were released from the impacted evaporite rich rocks resulting in sulphur aerosol-induced global cooling of >20°C for over three decades. For context, a global warming of >4.9°C is associated with full glacial to interglacial transition in the Pleistocene[153]. The impact-driven atmospheric compositional changes shifted the light spectral qualities and intensity for photosynthetic organisms on land and in the oceans[154]. Locally, the magnitude of aerosol-induced cooling was heterogenous, with the highest declines predicted for the tropics (>40°C) but less at high latitudes. Other elements potentially released from the impacted anhydrite rich rocks include calcium, sodium, magnesium and potassium: a melange that has been called 'plant fertilizer'[155].

Long- and short-term environmental changes in the aftermath of the asteroid impact resulted in geographically heterogenous plant extinction (see [21,156]). Wilf et al.[156] suggest the heterogeneity in

extinction intensity among land plants can be explained by climatic buffering of the impacts of climate winter and aerosol load. However, variable taxonomic resolution of fossil taxa, particularly among palynofloras, may mean that cryptic extinctions offer an alternative explanation[157] (Extended Table 2). Species extinction was over 50% within the best studied western North American macrofloras, but globally no plant family extinctions have been documented[156,158]. There was a 46% extinction of palynomorph species recorded from the tropical records of Colombia, significantly elevated extinction rates above background and a six-million-year-long recovery interval with evidence for substantial ecological and compositional changes in both palynofloras and macrofloras[155]. Angiosperm pollen increased in both relative abundance and frequency of occurrence in the earliest Paleogene, compared to latest Cretaceous samples[155]. A similar increase is also observed in New Zealand[159]. Ordination analysis of macrofossil records from western USA shows a significant compositional shift, indicative of ecosystem collapse[158] (Fig. 4). Extinctions of between 15 and 30% are recorded for New Zealand and North American palynofloras, respectively[21].

The latest Cretaceous was characterised by palynological provincialization[21] and only a few pollen fossil types were globally widespread, abundant, and diverse. Among these, *Aquilapollenites* (Fig. 1) and closely allied pollen were extirpated across their entire geographic range (including North America, Europe, Russia, Asia and Greenland, India) surviving only as a rare elements following the K-Pg boundary[160]. Other angiosperm taxa of unknown familial affinity that went extinct during or immediately after the end-Cretaceous include *Buttinia* and *Crassitricolporites*[161]. In the Indian intertrappean beds, *Aquilapollenites* diversity drops from ten to two species after the K-Pg boundary and pollen concentrations decreased from 6–50 per 200g in the Maastrichtian to a maximum of 2 per 200g in the Paleocene[160]. Although the taxonomic affinities of *Aquilapollenites* remains uncertain[162], their potential link to Santalales/Loranthaceae is intriguing because of the modern association of these clades with plant hemiparasitism. Hemiparasites are mixotrophic, meaning that they obtain carbon via their own photosynthesis and/or via parasitising that of their host[163]. As a functional group, they can also cost-effectively extract nutrients and water from their hosts[164]. Ecologically, hemiparasites are considered ecosystem engineers or keystone species because they can alter the structure, diversity and evenness of ecosystems by suppressing the dominance of their hosts, allowing sub-dominant taxa to coexist[164,165]. If *Aquilapollenites*-type pollen represents a widely distributed, hemiparasite-rich group, then extinction of their hosts could have driven their extinction indirectly or, alternatively, the ecological decline of this pollen group could have changed ecosystem function by releasing resource pressure on their hosts. Alternatively, *Aquilapollenites*-type 'triprojectate' pollen is usually inferred to be dispersed by insects[166], and its significant reduction could have been caused to the selective extirpation of their insect vectors[167]. Regardless of the proximate cause(s), their global decline signifies the collapse of the Late Cretaceous *Aquilapollenites* biome (Fig. 1) following the IUCN ecosystem criteria despite not going globally extinct as a higher taxonomic group.

One of the most consistent and remarkable global signatures of the end-Cretaceous is a geologically short-term but significant increase in the relative abundance of fern spores[21], termed a 'fern spike'. The fern acme is followed by homogeneous, low-diversity floras across western North American sites but with some notable exceptions that are classed as potential refugia (e.g., Castlerock Flora)[168]. In Patagonian[169] and New Zealand[170] floras, no significant extinctions are recorded but many species are lost from the floras precisely around the time of the asteroid impact and replaced by short-term Cheirolepidiaceae conifer or fern dominance, respectively. This suggests rapid ecosystem collapse, but equally rapid recovery of novel ecosystem compositions, patterns similar to those illustrated from Montana, USA[158] (Fig. 4). In the Neotropics, the end-Cretaceous extinction led to the 'birth' of Neotropical rainforest reflected by the replacement of mixed open canopy gymnosperm and angiosperm forests by angiosperm dominated systems with a closed canopy structure and a taxonomic composition very similar to that of contemporary wet tropical forests[155,156]. Although, there are no family-level global extinctions recorded for the end-Cretaceous[2], the permanent compositional and functional changes[155] provide robust evidence for Neotropical forest ecosystem collapse according to the IUCN Red List of Ecosystems criteria.

Summary

While plants appear to be more resilient to extinction than animals in both modern[171] and prehistoric[2,19] contexts, we argue that fossil plant diversity and elevation of extinction rates alone are insufficient gauges of the impacts of mass extinction events on plants. This stems from inherent biases in the fossil record, in addition to issues that arise from mapping modern extinction risk diagnostic criteria onto fossils. Our reviews of the Late Devonian, Mid-Late Pennsylvanian boundary, end-Permian, end-Triassic and end-Cretaceous plant fossil records, has revealed compelling evidence for widespread ecosystem collapse (Figs 1, 4, Extended Table 3) associated with each of these episodes of extreme environmental change. We have reviewed the evidence for, and against, the presence of plant ‘mass extinction’ at five target intervals in Earth history using abundance-loss criteria (Fig. 4) and provided a summary of findings (Extended Table 3) and a re-analysis (Fig. 3). We argue that applying principles and concepts from the IUCN Red List of Ecosystems model to palaeobiology to draw inferences about ecosystem collapse may be a more fruitful, or at least a complementary, framework to draw parallels and lessons from past plant extinction intervals (Extended Table 1) rather than endlessly debating whether or not an event constitutes a ‘mass extinction’ (Extended Table 2).

By leveraging the fossil record’s unique, long-term perspective as a gauge of natural ecosystem resilience and variability, this is the first time, to our knowledge, that alternative hypotheses of the IUCN ecosystem collapse model[18,22] (Extended Table 1) have been tested (Fig. 4). We show that ecosystem collapse during four of the five examined events is characterized by a transition to a distinct and novel ecosystem post-collapse rather than by an expansion of the antecedent ecospace (Fig. 4, Extended Table 1). Moreover, the multivariate ecospace analysis of relative abundance data demonstrated that post-collapse ecosystems were expanded compared to their pre-collapsed states (Fig. 4). This pattern

was consistent for all examined plant extinction intervals, suggesting a state of significant instability in terms of community composition for up to millions of years following collapse. The expanded ecospaces likely resulted from some combination of population changes among survivor taxa, adaptive radiation following niche vacancy, and immigration from refugia of different palaeo-latitudes or -altitudes, all to be tested and explored further in future work.

In all events considered here, post-collapse ecosystems are dominated by plant groups different from those that preceded the collapse, reflecting permanent shifts in ecospace (Fig. 4). Although all events involve a range of extinction severity (Fig. 3) with evidence of regional extirpation (MLPB, ETE, ECE) to global extinction (LDE, EPE) of geographically widespread, species-rich clades (Fig. 1), all show comparable long-term ecological impacts (Fig. 4). Thus, the notion of 'ecosystem recovery' is misleading, as it might imply the return of pre-collapse dominants. This distinction is important today: if we assume that ecosystems and the roles of their primary components will recover, this will foster complacency amid rapid contemporary environmental change.

There is much interest in using the palaeobiological record to identify early warning signs of mass extinction, and to highlight predictors of species extinction risk that may be useful for modern conservation science. We have not been successful in identifying early warning signs of plant mass extinction beyond reinforcing the message that extreme climate and atmospheric changes reliably lead to ecosystem collapse (Figs 2, 4). Further, in agreement with some contemporary conservation studies[172], no universal set of functional or ecological traits appear to increase or diminish extinction risk at all the extinction events reviewed here, beyond the observation that every event was marked by a geologically short interval of spore-producing plant dominance (e.g., fern or lycophyte abundance 'spikes') and a relative paucity of woody plants (trees). We note however that quantitative extinction risk predictor studies similar to those undertaken for marine invertebrates[173] are needed for plants.

An interesting finding associated with all of the reviewed extinction intervals is that they break some predictions of contemporary plant (angiosperm) extinction risk: that taxa with wide geographical ranges have relatively low extinction risk[146]. We have shown multiple examples from different biogeographic distributions (Fig. 1) and climate contexts (Fig. 2) that dominant taxa which defined their palaeoecosystems and/or had wide geographical distributions went extinct at plant mass extinction boundaries in the past. Similar results have been shown for marine invertebrates at mass extinction boundaries[6]. On land, these were often (Fig. 1A, B, C)—but not always (Fig. 1D, E)—trees that likely constituted a large proportion of terrestrial biomass. Equally, rare and sub-dominant taxa within the palaeofloras became the new dominants within the post-collapsed ecosystems for some of the extinction events studied (e.g., end-Triassic[24]).

Therefore, there are important lessons that can be derived from this review. Firstly, it highlights the overwhelming importance of IUCN red-listed species which are currently ecologically rare and non-competitive, yet they may be predisposed to thrive under projected climate changes and take on a prominent ecological role in future novel ecosystems if they are afforded appropriate protections. At

present, the fossil record has not yet provided clear, recurrent patterns of plant traits that offer resilience to projected global environmental changes, but this would be a fruitful avenue for future research. Secondly, and equally important: we cannot be complacent about the conservation of abundant, widely distributed taxa, since there is ample evidence from the deep past that these too are vulnerable to environmental change-driven extinction.

Methods

Palaeobiogeography

Data (Fig. 1) were collected from the Palaeobiology Database (paleobiodb.org), collected on 06/12/2025. Coordinate rotations of occurrence localities and palaeogeographic reconstructions performed using GPlates[174] with the PaleoMAP v3 plate model[175]. Note: fossil distributions have not been filtered for erroneous records[176].

Extinction rates

Background extinction rate regression line (Fig. 3) was calculated from the dataset of Cascales-Miñana & Cleal[2] but recalculated using the latest chronostratigraphic stage durations[177] (Supp. Table 2). This study is not intended as a revision of fossil affinities and taxon ranges (e.g., the Cenozoic extinction of potential Umkomasiaceae[178]), nor have we updated this dataset with more recent fossil localities or occurrences. Stages with no extinctions were included, and all families were included, regardless of their rarity. Post-Cretaceous stages were excluded to prevent bias from the inclusion of young families, which are unlikely to have yet gone extinct (even owing to 'background' influences). Therefore, end-Cretaceous extinction rates cannot be illustrated here. In the absence of independent exclusion criteria, the dataset from which the regression line was calculated included the events with peak extinction rates, following Cascales-Miñana & Cleal[2], but in contrast to Raup & Sepkoski[1].

Ordination analysis

Changes in ecospace were visualized as two-dimensional ordinations of fossil plant abundance data using non-metric multidimensional scaling (NMDS) with the Bray-Curtis dissimilarity index[179]. NMDS has been applied previously to fossil plant floras[92,180–182]. For all but one event (Mid-Late Pennsylvanian Boundary, MLPB), we utilized previously published NMDS ordinations (see Fig. 4 for sources). The MLPB ordination was based on the dataset compiled by Phillips et al.[183] for the Illinois Basin, USA. Pre-collapse data include all Desmoinesian Stage samples (prior to the MLPB), post-collapse data include all Missourian Stage samples (Supp. Table 3). Prior to ordination in two dimensions, the dataset underwent Hellinger transformation[184] to reduce the inordinate influence of very high or zero values (stress = 0.1271). Ordination conducted in PAST version 4.17[185]. For valid comparisons, pre- and post-event sampling intervals should be considered, and standardized where possible; when absolute age durations were unavailable, interval lengths were approximated by stratigraphic thicknesses. Respective pre- and

post-event durations/thicknesses were as follows: 312.6–305.7 Ma and 305.7–303.6 Ma for the MLPB; c. 95 m (pre-event), c. 23 m (early post-event) and c. 541 m (late post-event) for the end-Permian; c. 53 m and c. 96 m for the end-Triassic (maximum thicknesses across the two sampled localities); and c. 54 m and c. 38 m for the end-Cretaceous.

References

1. Raup, D. M. & Sepkoski, J. J. Mass extinctions in the marine fossil record. *Science* **215**, 1501–1503 (1982).
2. Cascales-Miñana, B. & Cleal, C. J. The plant fossil record reflects just two great extinction events. *Terra Nova* **26**, 195–200 (2014).
3. Wiens, J. J. & Saban, K. E. Questioning the sixth mass extinction. *Trends Ecol. Evol.* **40**, 375–384 (2025).
4. International Union of the Conservation of Nature. *IUCN Red List Categories and Criteria: Version 3.1. Second Edition*. 32 pp. (International Union for Conservation of Nature, Gland, Switzerland, 2012).
5. Keith, D. Red listing: Deciding which species are at risk. *Significance* **6**, 100–104 (2009).
6. Jablonski, D. Extinctions: A paleontological perspective. *Science* **253**, 754–757 (1991).
7. Foote, M. Origination and extinction components of taxonomic diversity: General problems. *Paleobiology* **26**, 74–102 (2000).
8. Burgman, M. A., Ferson, S. & Akçakaya, H. R. *Risk Assessment in Conservation Biology*. (Chapman and Hall, London, 1993).
9. Dale, V. H. *et al.* Climate change and forest disturbances. *BioScience* **51**, 723–734 (2001).
10. Brook, B. W. *et al.* Integrating bioclimate with population models to improve forecasts of species extinctions under climate change. *Biol. Lett.* **5**, 723–725 (2009).
11. Grime, J. P. Benefits of plant diversity to ecosystems: immediate, filter and founder effects. *J. Ecol.* **86**, 902–910 (1998).
12. Smith, M. D. & Knapp, A. K. Dominant species maintain ecosystem function with non-random species loss. *Ecol. Lett.* **6**, 509–517 (2003).
13. Genung, M. A., Fox, J. & Winfree, R. Species loss drives ecosystem function in experiments, but in nature the importance of species loss depends on dominance. *Glob. Ecol. Biogeogr.* **29**, 1531–1541 (2020).
14. Tilman, D. & El Haddi, A. Drought and biodiversity in grasslands. *Oecologia* **89**, 257–264 (1992).
15. Collins, S. L. & Steinauer, E. M. Disturbance, diversity, and species interactions in tallgrass prairie. in *Grassland Dynamics* (eds Knapp, A. K., Briggs, J. M., Hartnett, D. C. & Collins, S. L.) 140–156 (Oxford University Press, New York, 1998). doi:10.1093/oso/9780195114867.003.0009.
16. Bar-On, Y. M., Phillips, R. & Milo, R. The biomass distribution on Earth. *Proc. Natl. Acad. Sci. U. S. A.* **115**, 6506–6511 (2018).

17. Hordijk, I. *et al.* Dominance and rarity in tree communities across the globe: Patterns, predictors and threats. *Glob. Ecol. Biogeogr.* **33**, e13889 (2024).
18. International Union of the Conservation of Nature. *Guidelines for the Application of IUCN Red List of Ecosystems Categories and Criteria: Version 2.0*. (International Union for Conservation of Nature, Gland, Switzerland, 2024). doi:10.2305/CJDF9122.
19. McElwain, J. C. & Punyasena, S. W. Mass extinction events and the plant fossil record. *Trends Ecol. Evol.* **22**, 548–557 (2007).
20. McGhee, G. R., Clapham, M. E., Sheehan, P. M., Bottjer, D. J. & Droser, M. L. A new ecological-severity ranking of major Phanerozoic biodiversity crises. *Palaeogeogr. Palaeoclimatol. Palaeoecol.* **370**, 260–270 (2013).
21. Vajda, V. & Bercovici, A. The global vegetation pattern across the Cretaceous–Paleogene mass extinction interval: A template for other extinction events. *Glob. Planet. Change* **122**, 29–49 (2014).
22. Keith, D. A. *et al.* The IUCN Red List of Ecosystems: Motivations, challenges, and applications. *Conserv. Lett.* **8**, 214–226 (2015).
23. Holland, S. M. The stratigraphy of mass extinctions and recoveries. *Annu. Rev. Earth Planet. Sci.* **48**, 75–97 (2020).
24. McElwain, Popa, M. E., Hesselbo, S. P., Haworth, M. & Surlyk. Macroecological responses of terrestrial vegetation to climatic and atmospheric change across the Triassic/Jurassic boundary in East Greenland. *Paleobiology* **33**, 547–573 (2007).
25. Knetge, A. B. *et al.* Census collection of two fossil plant localities in Jameson Land, East Greenland supports regional ecological turnover and diversity loss at the end-Triassic mass extinction. *Palaeogeogr. Palaeoclimatol. Palaeoecol.* **679**, 113266 (2025).
26. Mays, C., Amores, M. & Mays, A. Field-of-view subsampling: A novel 'exotic marker' method for absolute abundances, validated by simulation and microfossil case studies. *PLOS One* **20**, e0320887 (2025).
27. Mays, C., Tyson, R. V. & Hren, M. T. Measures of prehistoric terrestrial net ecosystem productivity and carbon sink function. *Earth-Sci. Rev.* **270**, 105222 (2025).
28. Jackson, D. A. Compositional data in community ecology: the paradigm or peril of proportions? *Ecology* **78**, 929–940 (1997).
29. Carmichael, S. K., Waters, J. A., Königshof, P., Suttner, T. J. & Kido, E. Paleogeography and paleoenvironments of the Late Devonian Kellwasser event: A review of its sedimentological and geochemical expression. *Glob. Planet. Change* **183**, 102984 (2019).
30. Kaiser, S. I., Aretz, M. & Becker, R. T. The global Hangenberg Crisis (Devonian–Carboniferous transition): review of a first-order mass extinction. in *Devonian Climate, Sea Level and Evolutionary Events* (eds Becker, R. T., Königshof, P. & Brett, C. E.) 387–437 (Geological Society, London, 2016).
31. Algeo, T. J. & Shen, J. Theory and classification of mass extinction causation. *Natl. Sci. Rev.* **11**, nwad237 (2024).

32. Judd, E. J. *et al.* A 485-million-year history of Earth's surface temperature. *Science* **385**, eadk3705 (2024).
33. Bond, D. P. G. & Wignall, P. B. The role of sea-level change and marine anoxia in the Frasnian–Famennian (Late Devonian) mass extinction. *Palaeogeogr. Palaeoclimatol. Palaeoecol.* **263**, 107–118 (2008).
34. Kaiser, S. I., Becker, R. T., Steuber, T. & Aboussalam, S. Z. Climate-controlled mass extinctions, facies, and sea-level changes around the Devonian–Carboniferous boundary in the eastern Anti-Atlas (SE Morocco). *Palaeogeogr. Palaeoclimatol. Palaeoecol.* **310**, 340–364 (2011).
35. Goddéris, Y. & Joachimski, M. M. Global change in the Late Devonian: modelling the Frasnian–Famennian short-term carbon isotope excursions. *Palaeogeogr. Palaeoclimatol. Palaeoecol.* **202**, 309–329 (2004).
36. Edwards, D., Fairon-Demaret, M. & Berry, C. M. Plant megafossils in Devonian stratigraphy: a progress report. in *Subcommission on Devonian Stratigraphy: Fossil Groups Important for Boundary Definition* (ed. Bultynck, P.) 25–37 (E. Schweizerbart Science Publishers, Stuttgart, 2000).
37. Taherian, F., Vaez-Javadi, F. & Vaziri, S. H. Miospores from the Upper Devonian and lowermost Carboniferous strata of the Khoshyeilagh area, northeastern Alborz, Iran. *Palynology* **46**, 1–16 (2022).
38. Gastaldo, R. A. *et al.* Enigmatic fossil plants with three-dimensional, arborescent-growth architecture from the earliest Carboniferous of New Brunswick, Canada. *Curr. Biol.* **34**, 781-792.e3 (2024).
39. Maziane, N., Higgs, K. T. & Streel, M. Biometry and paleoenvironment of *Retispora lepidophyta* (Kedo) Playford 1976 and associated miospores in the latest Famennian nearshore marine facies, eastern Ardenne (Belgium). *Rev. Palaeobot. Palynol.* **118**, 211–226 (2002).
40. Stein, W. E. *et al.* Mid-Devonian *Archaeopteris* roots signal revolutionary change in earliest fossil forests. *Curr. Biol.* **30**, 421–431 (2020).
41. Meyer-Berthaud, B., Scheckler, S. E. & Bousquet, J. The development of *Archaeopteris*: new evolutionary characters from the structural analysis of an early Famennian trunk from southeast Morocco. *Am. J. Bot.* **87**, 456–468 (2000).
42. Cressler, W. L. Plant paleoecology of the Late Devonian Red Hill locality, north-central Pennsylvania, an *Archaeopteris*-dominated wetland plant community and early tetrapod site. in *Wetlands through Time* 79–102 (Geological Society of America, 2006). doi:10.1130/2006.2399(04).
43. Decombeix, A.-L., Meyer-Berthaud, B. & Galtier, J. Transitional changes in arborescent lignophytes at the Devonian–Carboniferous boundary. *J. Geol. Soc.* **168**, 547–557 (2011).
44. Marshall, J. E. A. A terrestrial Devonian-Carboniferous boundary section in East Greenland. *Palaeobiodiversity Palaeoenvironments* **101**, 541–559 (2021).
45. Prestianni, C., Sautois, M. & Denayer, J. Disrupted continental environments around the Devonian-Carboniferous Boundary: introduction of the *tener* event. *Geol. Belg.* **19**, 135–145 (2016).
46. Marshall, J. E. A., Lakin, J., Troth, I. & Wallace-Johnson, S. M. UV-B radiation was the Devonian-Carboniferous boundary terrestrial extinction kill mechanism. *Sci. Adv.* **6**, aba0768 (2020).

47. Van Veen, P. M. Aspects of Late Devonian and early carboniferous palynology of southern Ireland. V. The change in composition of palynological assemblages at the Devonian-Carboniferous boundary. *Rev. Palaeobot. Palynol.* **34**, 67–97 (1981).
48. Balme, B. E. Fossil *in situ* spores and pollen grains: An annotated catalogue. *Rev. Palaeobot. Palynol.* **87**, 81–323 (1995).
49. McElwain, J. C. *et al.* Functional traits of fossil plants. *New Phytol.* **242**, 392–423 (2024).
50. Fields, B. D. *et al.* Supernova triggers for end-Devonian extinctions. *Proc. Natl. Acad. Sci. U. S. A.* **117**, 21008–21010 (2020).
51. Racki, G. A volcanic scenario for the Frasnian–Famennian major biotic crisis and other Late Devonian global changes: More answers than questions? *Glob. Planet. Change* **189**, 103174 (2020).
52. Marshall, J. E. A., Astin, T. R., Tel'nova, O. P. & Gaca, P. Terrestrial palaeoclimate, mercury, atmospheric CO_2 and land plants through the Late Devonian mass extinction. *J. Geol. Soc.* **182**, jgs2024-187 (2025).
53. Phillips, T. L. & Galtier, J. Evolutionary and ecological perspectives of Late Paleozoic ferns. *Rev. Palaeobot. Palynol.* **135**, 165–203 (2005).
54. Galtier, J., Meyer-Berthaud, B. & Rowe, N. P. Tournaisian plants from the 'Lydiennes' Formation of the Montagne Noire (France). *Cour. Forschungsinstitut Senckenberg* **100**, 109–117 (1988).
55. Hübers, M., Bomfleur, B., Krings, M., Pott, C. & Kerp, H. A reappraisal of Mississippian (Tournaisian and Visean) adpression floras from central and northwestern Europe. *Zitteliana A* **54**, 39–52 (2014).
56. Galtier, J. *Pitus*, a giant tree of the Early Carboniferous time. in *Secrets of Petrified Plants–Fascination from Millions of Years* (eds Dernbach, U. & Tidwell, W. D.) 34–37 (D'oro Publishers, Heppenheim, 2002).
57. DiMichele, W. A., Phillips, T. L. & Pfefferkorn, H. W. Paleoecology of Late Paleozoic pteridosperms from tropical Euramerica. *J. Torrey Bot. Soc.* **133**, 83–118 (2006).
58. Myrow, P. M. *et al.* High-precision U-Pb age and duration of the latest Devonian (Famennian) Hangenberg Event, and its implications. *Terra Nova* **26**, 222–229 (2014).
59. Percival, L. M. E. *et al.* Precisely dating the Frasnian–Famennian boundary: implications for the cause of the Late Devonian mass extinction. *Sci. Rep.* **8**, 9578 (2018).
60. Silvestro, D., Cascales-Miñana, B., Bacon, C. D. & Antonelli, A. Revisiting the origin and diversification of vascular plants through a comprehensive Bayesian analysis of the fossil record. *New Phytol.* **207**, 425–436 (2015).
61. Prestianni, C. & Gerrienne, P. Early seed plant radiation: an ecological hypothesis. *Geol. Soc. Lond. Spec. Publ.* **339**, 71–80 (2010).
62. Prestianni, C. *et al.* Early seed plants from western Gondwana: Paleobiogeographical and ecological implications based on Tournaisian (lower Carboniferous) records from Argentina. *Palaeogeogr. Palaeoclimatol. Palaeoecol.* **417**, 210–219 (2015).

63. Montañez, I. P. *et al.* Climate, pCO_2 and terrestrial carbon cycle linkages during late Palaeozoic glacial–interglacial cycles. *Nat. Geosci.* **9**, 824–828 (2016).
64. DiMichele, W. A. *et al.* Kasimovian floristic change in tropical wetlands and the Middle–Late Pennsylvanian Boundary Event. *Geol. Soc. Lond. Spec. Publ.* **535**, 293–335 (2023).
65. DiMichele, W. A. Wetland-dryland vegetational dynamics in the Pennsylvanian ice age tropics. *Int. J. Plant Sci.* **175**, 123–164 (2014).
66. Falcon-Lang, H. J. & DiMichele, W. A. What happened to the coal forests during the Pennsylvanian glacial phases? *PALAIOS* **25**, 611–617 (2010).
67. Pfefferkorn, H. W., Gastaldo, R. A., DiMichele, W. A. & Phillips, T. L. Pennsylvanian tropical floras from the United States as a record of changing climate. In *Resolving the Late Paleozoic Ice Age in Time and Space* vol. 441 305–316 (Geological Society of America, 2008).
68. Kosanke, R. M. & Cecil, C. B. Late Pennsylvanian climate changes and palynomorph extinctions. *Rev. Palaeobot. Palynol.* **90**, 113–140 (1996).
69. DiMichele, W. A. & Phillips, T. L. Climate change, plant extinctions and vegetational recovery during the Middle-Late Pennsylvanian transition: The case of tropical peat-forming environments in North America. *Geol. Soc. Lond. Spec. Publ.* **102**, 201–221 (1997).
70. Tian, B. & Guo, G. A new species of lepidodendroid fructification-*Achlamydocarpon sinensis*. *Acta Bot. Sin.* **29**, 218–222 (1987).
71. Dimitrova, T. Kh. & Cleal, C. J. Palynological evidence for late Westphalian–early Stephanian vegetation change in the Dobrudzha Coalfield, NE Bulgaria. *Geol. Mag.* **144**, 513–524 (2007).
72. DiMichele, W. A., Montañez, I. P., Poulsen, C. J. & Tabor, N. J. Climate and vegetational regime shifts in the late Paleozoic ice age earth. *Geobiology* **7**, 200–226 (2009).
73. Matthaeus, W. J. *et al.* A systems approach to understanding how plants transformed Earth's environment in deep time. *Annu. Rev. Earth Planet. Sci.* **51**, 551–580 (2023).
74. Rosenau, N. A., Tabor, N. J., Elrick, S. D. & Nelson, W. J. Polygenetic history of paleosols in Middle-Upper Pennsylvanian cyclothems of the Illinois Basin, U.S.A.: Part II. Integrating geomorphology, climate, and glacioeustasy. *J. Sediment. Res.* **83**, 637–668 (2013).
75. Bashforth, A. R. *et al.* The environmental implications of upper Paleozoic plant-fossil assemblages with mixtures of wetland and drought-tolerant taxa in tropical Pangea. *Geobios* **68**, 1–45 (2021).
76. Lucas, S. G. Middle to Late Pennsylvanian tetrapod evolution: the Kasimovian bottleneck. *Geol. Soc. Lond. Spec. Publ.* **535**, 481–497 (2023).
77. DiMichele, W. A., Mamay, S. H., Chaney, D. S., Hook, R. W. & John Nelson, W. An early Permian flora with late Permian and Mesozoic affinities from north-central Texas. *J. Paleontol.* **75**, 449–460 (2001).
78. Krings, M., Kerp, H., Taylor, T. N. & Taylor, E. L. How Paleozoic vines and lianas got off the ground: On scrambling and climbing Carboniferous–Early Permian pteridosperms. *Bot. Rev.* **69**, 204–224 (2003).

79. Cheesman, A. W., Duff, H., Hill, K., Cernusak, L. A. & McInerney, F. A. Isotopic and morphologic proxies for reconstructing light environment and leaf function of fossil leaves: a modern calibration in the Daintree Rainforest, Australia. *Am. J. Bot.* **107**, 1165–1176 (2020).
80. Matthaeus, W. J. *et al.* Vegetation turnovers reduced water availability during the last icehouse. *Glob. Ecol. Biogeogr.* **34**, e70117 (2025).
81. Fang, Q. *et al.* Synchronizing climate-carbon cycle heartbeats in the Phanerozoic vegetated icehouses. *Nat. Commun.* **16**, 9196 (2025).
82. Stanley, S. M. Estimates of the magnitudes of major marine mass extinctions in earth history. *Proc. Natl. Acad. Sci.* **113**, E6325–E6334 (2016).
83. Fielding, C. R. *et al.* Age and pattern of the southern high-latitude continental end-Permian extinction constrained by multiproxy analysis. *Nat. Commun.* **10**, 385 (2019).
84. Chu, D. *et al.* Ecological disturbance in tropical peatlands prior to marine Permian-Triassic mass extinction. *Geology* **48**, 288–292 (2020).
85. Xiong, C. *et al.* Plant resilience and extinctions through the Permian to Middle Triassic on the North China Block: A multilevel diversity analysis of macrofossil records. *Earth-Sci. Rev.* **223**, 103846 (2021).
86. Song, H., Wignall, P. B., Tong, J. & Yin, H. Two pulses of extinction during the Permian–Triassic crisis. *Nat. Geosci.* **6**, 52–56 (2013).
87. Burgess, S. D., Bowring, S. & Shen, S.-Z. High-precision timeline for Earth's most severe extinction. *Proc. Natl. Acad. Sci. U. S. A.* **111**, 3316–3321 (2014).
88. Lyon, C. *et al.* Climate change research and action must look beyond 2100. *Glob. Change Biol.* **28**, 349–361 (2021).
89. Wu, Q. *et al.* The terrestrial end-Permian mass extinction in the paleotropics postdates the marine extinction. *Sci. Adv.* **10**, eadi7284 (2024).
90. Bomfleur, B., Blomenkemper, P., Kerp, H. & McLoughlin, S. Polar regions of the Mesozoic-Paleogene greenhouse world as refugia for relict plant groups. in *Transformative Paleobotany: Papers to Commemorate the Life and Legacy of Thomas N. Taylor* (eds Krings, Harper, C. J., Cuneo, N. R. & Rothwell, G. W.) 593–611 (Academic Press, Cambridge, 2018).
91. McLoughlin, S., Lindström, S. & Drinnan, A. N. Gondwanan floristic and sedimentological trends during the Permian-Triassic transition: new evidence from the Amery Group, northern Prince Charles Mountains, East Antarctica. *Antarct. Sci.* **9**, 281–298 (1997).
92. Amores, M., Frank, T. D., Fielding, C. R., Hren, M. T. & Mays, C. Age-controlled south polar floral trends show a staggered Early Triassic gymnosperm recovery following the end-Permian event. *GSA Bull.* **137**, 3255–3282 (2025).
93. Wignall, P. B. & Bond, D. P. G. The great catastrophe: causes of the Permo-Triassic marine mass extinction. *Natl. Sci. Rev.* **11**, nwad273 (2024).

94. Burgess, S. D. & Black, B. A. The anatomy and lethality of the Siberian Traps Large Igneous Province. *Annu. Rev. Earth Planet. Sci.* **53**, 567–594 (2025).
95. Sun, Y. D. *et al.* Lethally hot temperatures during the Early Triassic greenhouse. *Science* **338**, 366–370 (2012).
96. Frank, T. D. *et al.* Pace, magnitude, and nature of terrestrial climate change through the end Permian extinction in southeastern Gondwana. *Geology* **49**, 1089–1095 (2021).
97. Smith, R. M. H. & Botha-Brink, J. Anatomy of a mass extinction: Sedimentological and taphonomic evidence for drought-induced die-offs at the Permo-Triassic boundary in the main Karoo Basin, South Africa. *Palaeogeogr. Palaeoclimatol. Palaeoecol.* **396**, 99–118 (2014).
98. Li, J., Gastaldo, R. A., Neveling, J. & Geissman, J. W. Siltstones across the *Daptocephalus* (*Dicynodon*) and *Lystrosaurus* assemblage zones, Karoo Basin, South Africa, show no evidence for aridification. *J. Sediment. Res.* **87**, 653–671 (2017).
99. Mays, C. & McLoughlin, S. End-Permian burnout: The role of Permian-Triassic wildfires in extinction, carbon cycling and environmental change in eastern Gondwana. *Palaios* **37**, 292–317 (2022).
100. Black, B. A. *et al.* Systemic swings in end-Permian climate from Siberian Traps carbon and sulfur outgassing. *Nat. Geosci.* **11**, 949–954 (2018).
101. Benca, J. P., Duijnstee, I. A. P. & Looy, C. V. UV-B–induced forest sterility: Implications of ozone shield failure in Earth's largest extinction. *Sci. Adv.* **4**, 10 (2018).
102. Liu, F. *et al.* Dying in the sun: Direct evidence for elevated UV-B radiation at the end-Permian mass extinction. *Sci. Adv.* **9**, eabo6102 (2023).
103. Black, B. A., Lamarque, J.-F., Shields, C. A., Elkins-Tanton, L. T. & Kiehl, J. T. Acid rain and ozone depletion from pulsed Siberian Traps magmatism. *Geology* **42**, 67–70 (2014).
104. Grasby, S. E., Liu, X., Yin, R., Ernst, R. E. & Chen, Z. Toxic mercury pulses into late Permian terrestrial and marine environments. *Geology* **48**, 830–833 (2020).
105. Shen, J. *et al.* Mercury evidence from southern Pangea terrestrial sections for end-Permian global volcanic effects. *Nat. Commun.* **14**, 6 (2023).
106. Rees, P. M. Land-plant diversity and the end-Permian mass extinction. *Geology* **30**, 827–830 (2002).
107. Schneebeli-Hermann, E. & Galasso, F. Resilient gymnosperms: reassessing floral dynamics at the Permian–Triassic extinction in Meishan. *Rev. Palaeobot. Palynol.* **341**, 105373 (2025).
108. Nowak, H., Schneebeli-Hermann, E. & Kustatscher, E. No mass extinction for land plants at the Permian–Triassic transition. *Nat. Commun.* **10**, 384 (2019).
109. Cascales-Miñana, B., Diez, J. B., Gerrienne, P. & Cleal, C. J. A palaeobotanical perspective on the great end-Permian biotic crisis. *Hist. Biol.* **28**, 1066–1074 (2016).
110. Mays, C. *et al.* Refined Permian–Triassic floristic timeline reveals early collapse and delayed recovery of south polar terrestrial ecosystems. *GSA Bull.* **132**, 1489–1513 (2020).
111. Xu, Z. *et al.* Early Triassic super-greenhouse climate driven by vegetation collapse. *Nat. Commun.* **16**, 5400 (2025).

112. Xu, Z. *et al.* End Permian to Middle Triassic plant species richness and abundance patterns in South China: Coevolution of plants and the environment through the Permian–Triassic transition. *Earth-Sci. Rev.* **232**, 104136 (2022).
113. Looy, C. V., van Konijnenburg-van Cittert, J. H. A. & Duijnstee, I. A. P. Proliferation of isoëtalean lycophytes during the Permo-Triassic biotic crises: A proxy for the state of the terrestrial biosphere. *Front. Earth Sci.* **9**, 615370 (2021).
114. Nowak, H., Vérard, C. & Kustatscher, E. Palaeophytogeograhical patterns across the Permian–Triassic boundary. *Front. Earth Sci.* **8**, 613350 (2020).
115. Retallack, G. J., John J. Veevers & Ric Morante. Global coal gap between Permian–Triassic extinction and Middle Triassic recovery of peat-forming plants. *GSA Bull.* **108**, 195–207 (1996).
116. McLoughlin, S. *Glossopteris*: Insights into the architecture and relationships of an iconic Permian Gondwanan plant. *J. Bot. Soc. Bengal* **65**, 1–14 (2011).
117. Saxena, A., Cleal, C. J. & Singh, K. J. The Permian–Triassic boundary in Peninsular India and the extinction of the Glossopteridales. *Gondwana Res.* **137**, 318–330 (2025).
118. Wenchao, S. *et al.* Floral dynamics and ecological adaptations in the Lopingian gigantopterid rainforest of South China. *Rev. Palaeobot. Palynol.* **338**, 105335 (2025).
119. Zhang, H. *et al.* The terrestrial end-Permian mass extinction in South China. *Palaeogeogr. Palaeoclimatol. Palaeoecol.* **448**, 108–124 (2016).
120. Turner, H.-A., McLoughlin, S. & Mays, C. Comprehensive survey of Early to Middle Triassic Gondwanan floras reveals under-representation of plant-arthropod interactions. *Front. Ecol. Evol.* **12**, 1419254 (2024).
121. Fielding, C. R. *et al.* Sedimentology of the continental end-Permian extinction event in the Sydney Basin, eastern Australia. *Sedimentology* **68**, 30–62 (2021).
122. Hermann, E., Hochuli, P. A., Bucher, H. & Roohi, G. Uppermost Permian to Middle Triassic palynology of the Salt Range and Surghar Range, Pakistan. *Rev. Palaeobot. Palynol.* **169**, 61–95 (2012).
123. Retallack, G. J. Permian-Triassic life crisis on land. *Science* **267**, 77–80 (1995).
124. Looy, C. V., Twitchett, R. J., Dilcher, D. L., van Konijnenburg-van Cittert, J. H. A. & Visscher, H. Life in the end-Permian dead zone. *Proc. Natl. Acad. Sci. U. S. A.* **98**, 7879–7883 (2001).
125. Grauvogel-Stamm, L. & Ash, S. R. Recovery of the Triassic land flora from the end-Permian life crisis. *Comptes Rendus Palevol* **4**, 593–608 (2005).
126. Ouyang, S. & Utting, J. Palynology of Upper Permian and Lower Triassic rocks, Meishan, Changxing County, Zhejiang Province, China. *Rev. Palaeobot. Palynol.* **66**, 65–103 (1990).
127. Feng, Z. *et al.* From rainforest to herbland: New insights into land plant responses to the end-Permian mass extinction. *Earth-Sci. Rev.* **204**, 103153 (2020).
128. Barbacka, M. *et al.* Changes in terrestrial floras at the Triassic-Jurassic Boundary in Europe. *Palaeogeogr. Palaeoclimatol. Palaeoecol.* **480**, 80–93 (2017).

129. Herrera, F. *et al.* The presumed ginkgophyte *Umaltolepis* has seed-bearing structures resembling those of Peltaspermales and Umkomasiales. *Proc. Natl. Acad. Sci.* **114**, E2385–E2391 (2017).
130. Harris, T. M. The fossil flora of Scoresby Sound, East Greenland. Part 5: Stratigraphic relations of the plant beds. *Meddelelser Om Gronland* **112**, 1–114 (1937).
131. Lundblad, B. Rhaeto-liassic floras and their bearing on the stratigraphy of Triassic rocks. *Acta Univ. Stockh.* **8**, 83–102 (1959).
132. Fowell, S. J. & Olsen, P. E. Time calibration of Triassic/Jurassic microfloral turnover, eastern North America. *Tectonophysics* **222**, 361–369 (1993).
133. Jablonski, D. Extinctions in the fossil record. *Philos. Trans. R. Soc. B* **344**, 11–17 (1994).
134. Mander, L., Kürschner, W. M. & McElwain, J. C. An explanation for conflicting records of Triassic–Jurassic plant diversity. *Proc. Natl. Acad. Sci. U. S. A.* **107**, 15351–15356 (2010).
135. Bonis, N. R. & Kürschner, W. M. Vegetation history, diversity patterns, and climate change across the Triassic/Jurassic boundary. *Paleobiology* **38**, 240–264 (2012).
136. Lindström, S. Palynofloral patterns of terrestrial ecosystem change during the end-Triassic event – a review. *Geol. Mag.* **153**, 223–251 (2016).
137. Quiroz-Cabascango, D., Vajda, V., McLoughlin, S. & Niedźwiedzki, G. Earliest Jurassic plant assemblages from Sweden reveal a low-diversity ginkgoalean and cheirolepid flora dominating the post-extinction landscape. *Ann. Bot.* mcaf143 (2025) doi:10.1093/aob/mcaf143.
138. Steinthorsdottir, M., Woodward, F. I., Surlyk, F. & McElwain, J. C. Deep-time evidence of a link between elevated CO_2 concentrations and perturbations in the hydrological cycle via drop in plant transpiration. *Geology* **40**, 815–818 (2012).
139. Belcher, C. M. *et al.* Increased fire activity at the Triassic/Jurassic boundary in Greenland due to climate-driven floral change. *Nat. Geosci.* **3**, 426–429 (2010).
140. Soh, W. K. *et al.* Palaeo leaf economics reveal a shift in ecosystem function associated with the end-Triassic mass extinction event. *Nat. Plants* **3**, 17104 (2017).
141. Kürschner, W. M., Batenburg, S. J. & Mander, L. Aberrant *Classopollis* pollen reveals evidence for unreduced (2 *n*) pollen in the conifer family Cheirolepidiaceae during the Triassic–Jurassic transition. *Proc. R. Soc. B Biol. Sci.* **280**, 20131708 (2013).
142. Lindström, S. *et al.* Volcanic mercury and mutagenesis in land plants during the end-Triassic mass extinction. *Sci. Adv.* **5**, 13 (2019).
143. Vajda, V., McLoughlin, S., Slater, S. M., Gustafsson, O. & Rasmusson, A. G. The 'seed-fern' *Lepidopteris* mass-produced the abnormal pollen *Ricciisporites* during the end-Triassic biotic crisis. *Palaeogeogr. Palaeoclimatol. Palaeoecol.* **627**, 111723 (2023).
144. Li, L.-Q., Wang, Y.-D., Kürschner, W. M., Ruhl, M. & Vajda, V. Palaeovegetation and palaeoclimate changes across the Triassic–Jurassic transition in the Sichuan Basin, China. *Palaeogeogr. Palaeoclimatol. Palaeoecol.* **556**, 109891 (2020).

145. Zhou, N. *et al.* Pattern of vegetation turnover during the end-Triassic mass extinction: Trends of fern communities from South China with global context. *Glob. Planet. Change* **205**, 103585 (2021).
146. Bachman, S. P., Brown, M. J. M., Leão, T. C. C., Nic Lughadha, E. & Walker, B. E. Extinction risk predictions for the world's flowering plants to support their conservation. *New Phytol.* **242**, 797–808 (2024).
147. McElwain, J. C. Paleobotany and global change: Important lessons for species to biomes from vegetation responses to past global change. *Annu. Rev. Plant Biol.* **69**, 761–787 (2018).
148. Alvarez, L. W., Alvarez, W., Asaro, F. & Michel, H. V. Extraterrestrial cause for the Cretaceous–Tertiary extinction. *Science* **208**, 1095–1108 (1980).
149. Hildebrand, A. R. *et al.* Chicxulub Crater: A possible Cretaceous/Tertiary boundary impact crater on the Yucatán Peninsula, Mexico. *Geology* **19**, 867–871 (1991).
150. Schoene, B. *et al.* U-Pb constraints on pulsed eruption of the Deccan Traps across the end-Cretaceous mass extinction. *Science* **3636**, 862–866 (2019).
151. Morgan, J. V., Bralower, T. J., Brugger, J. & Wünnemann, K. The Chicxulub impact and its environmental consequences. *Nat. Rev. Earth Environ.* **3**, 338–354 (2022).
152. Artemieva, N., Morgan, J., & Expedition 364 Science Party. Quantifying the release of climate-active gases by large meteorite impacts with a case study of Chicxulub. *Geophys. Res. Lett.* **44**, 10180–10188 (2017).
153. Shakun, J. D. & Carlson, A. E. A global perspective on Last Glacial Maximum to Holocene climate change. *Quat. Sci. Rev.* **29**, 1801–1816 (2010).
154. Aguirre, J., Riding, R. & Braga, J. C. Late Cretaceous incident light reduction: evidence from benthic algae. *Lethaia* **33**, 205–213 (2000).
155. Carvalho, M. R. *et al.* Extinction at the end-Cretaceous and the origin of modern Neotropical rainforests. *Science* **372**, 63–68 (2021).
156. Wilf, P., Carvalho, M. R. & Stiles, E. The end-Cretaceous plant extinction: Heterogeneity, ecosystem transformation, and insights for the future. *Camb. Prisms Extinction* **1**, 10 (2023).
157. Mander, L. & Punyasena, S. W. On the taxonomic resolution of pollen and spore records of Earth's vegetation. *Int. J. Plant Sci.* **175**, 931–945 (2014).
158. Wilson Deibel, P. K., Wilson Mantilla, G. P. & Strömberg, C. A. E. Plant taxonomic turnover and diversity across the Cretaceous/Paleogene boundary in northeastern Montana. *Paleobiology* **50**, 608–626 (2024).
159. Prebble, J. G. *et al.* A 100 million year composite pollen record from New Zealand shows maximum angiosperm abundance delayed until Eocene. *Palaeogeogr. Palaeoclimatol. Palaeoecol.* **566**, 8 (2021).
160. Samant, B., Mohabey, D. M. & Paudayal, K. N. *Aquilapollenites* and other triprojectate pollen from the Late Cretaceous to Early Paleocene Deccan intertrappean deposits of India. *Palynology* **37**, 298–315 (2013).

161. Vajda-Santivanez, V. Miospores from Upper Cretaceous-Paleocene strata in northwestern Bolivia. *Palynology* **23**, 181–196 (1999).

162. Tekleva, M., Polevova, S., Bugdaeva, E., Markevich, V. & Sun, G. Three *Aquilapollenites* species from the late Maastrichtian of China: New data and comparisons. *Rev. Palaeobot. Palynol.* **282**, 104288 (2020).

163. Těšitel, J. & Těšitelová, T. Approaching a revolution in hemiparasitic plant biology? A commentary on 'Distinguishing carbon gains from photosynthesis and heterotrophy in C3-hemiparasite–C3-host-pairs'. *Ann. Bot.* **129**, i–ii (2022).

164. Těšitel, J., Plavcová, L. & Cameron, D. D. Interactions between hemiparasitic plants and their hosts: The importance of organic carbon transfer. *Plant Signal. Behav.* **5**, 1072–1076 (2010).

165. Phoenix, G. K. & Press, M. C. Effects of climate change on parasitic plants: the root hemiparasitic Orobanchaceae. *Folia Geobot.* **40**, 205–216 (2005).

166. McIver, E. E., Sweet, A. R. & Basinger, J. F. Sixty-five-million-year-old flowers bearing pollen of the extinct triprojectate complex—a Cretaceous-Tertiary boundary survivor. *Rev. Palaeobot. Palynol.* **70**, 77–88 (1991).

167. Schachat, S. R. & Labandeira, C. C. Are insects heading toward their first mass extinction? Distinguishing turnover from crises in their fossil record. *Ann. Entomol. Soc. Am.* **114**, 99–118 (2021).

168. Johnson, K. R. & Ellis, B. A tropical rainforest in Colorado 1.4 million years after the Cretaceous-Tertiary boundary. *Science* **296**, 2379–2383 (2002).

169. Barreda, V. D. *et al.* Cretaceous/Paleogene floral turnover in Patagonia: Drop in diversity, low extinction, and a *Classopollis* spike. *PLOS One* **7**, e52455 (2012).

170. Vajda, V. & McLoughlin, S. Fungal proliferation at the Cretaceous–Tertiary boundary. *Science* **303**, 1489 (2004).

171. Román-Palacios, C. & Wiens, J. J. Recent responses to climate change reveal the drivers of species extinction and survival. *Proc. Natl. Acad. Sci. U. S. A.* **117**, 4211–4217 (2020).

172. Davies, T. W. *et al.* Dominance, biomass and extinction resistance determine the consequences of biodiversity loss for multiple coastal ecosystem processes. *PLoS ONE* **6**, e28362 (2011).

173. Malanoski, C. M., Farnsworth, A., Lunt, D. J., Valdes, P. J. & Saupe, E. E. Climate change is an important predictor of extinction risk on macroevolutionary timescales. *Science* **383**, 1130–1134 (2024).

174. Müller, R. D. *et al.* GPlates: Building a virtual Earth through deep time. *Geochem. Geophys. Geosystems* **19**, 2243–2261 (2018).

175. Kocsis, Á. T. & Scotese, C. R. Mapping paleocoastlines and continental flooding during the Phanerozoic. *Earth-Sci. Rev.* **213**, 103463 (2021).

176. Jones, L. A. *et al.* Ten simple rules to follow when cleaning occurrence data in palaeobiology. *Palaeontology* **68**, e70028 (2025).

177. Cohen, K., Harper, D., Gibbard, P. & Car, N. The ICS international chronostratigraphic chart this decade. *Episodes* **48**, 105–115 (2025).
178. Slodownik, M., Hill, R. S. & McLoughlin, S. *Komlopteris*: A persistent lineage of post-Triassic corystosperms in Gondwana. *Rev. Palaeobot. Palynol.* **317**, 104950 (2023).
179. Bray, J. R. & Curtis, J. T. An ordination of the upland forest communities of Southern Wisconsin. *Ecol. Monogr.* **27**, 325–349 (1957).
180. Wing, S. L. & Currano, E. D. Plant response to a global greenhouse event 56 million years ago. *Am. J. Bot.* **100**, 1234–1254 (2013).
181. Korasidis, V. A. & Wing, S. L. Palynofloral change through the Paleocene-Eocene thermal maximum in the Bighorn Basin, Wyoming. *Paleoceanogr. Paleoclimatology* **38**, e2023PA004741 (2023).
182. Slater, S. M., Twitchett, R. J., Danise, S. & Vajda, V. Substantial vegetation response to Early Jurassic global warming with impacts on oceanic anoxia. *Nat. Geosci.* **12**, 462–467 (2019).
183. Phillips, T. L., Peppers, R. A., Avcin, M. J. & Laughnan, P. F. Fossil plants and coal: Patterns of change in Pennsylvanian coal swamps of the Illinois Basin. *Science* **184**, 1367–1369 (1974).
184. Legendre, P. & Gallagher, E. D. Ecologically meaningful transformations for ordination of species data. *Oecologia* **129**, 271–280 (2001).
185. Hammer, Ø., Harper, D. A. T. & Ryan, P. D. PAST: Paleontological statistics software package for education and data analysis. *Palaeontol. Electron.* **4**, 9 (2001).
186. Bond, D. P. G. & Grasby, S. E. On the causes of mass extinctions. *Palaeogeogr. Palaeoclimatol. Palaeoecol.* **478**, 3–29 (2017).
187. Courtillot, V., Jaeger, J. J., Yang, Z., Feraud, G. & Hofmann, C. The influence of continental flood basalts on mass extinctions: Where do we stand? in *The Cretaceous-Tertiary Event and Other Catastrophes in Earth History* 513–525 (Geological Society of America, 1996). doi:10.1130/0-8137-2307-8.513.
188. Schmitz, M. D. & Davydov, V. I. Quantitative radiometric and biostratigraphic calibration of the Pennsylvanian-Early Permian (Cisuralian) time scale and pan-Euramerican chronostratigraphic correlation. *Geol. Soc. Am. Bull.* **124**, 549–577 (2012).

Figures

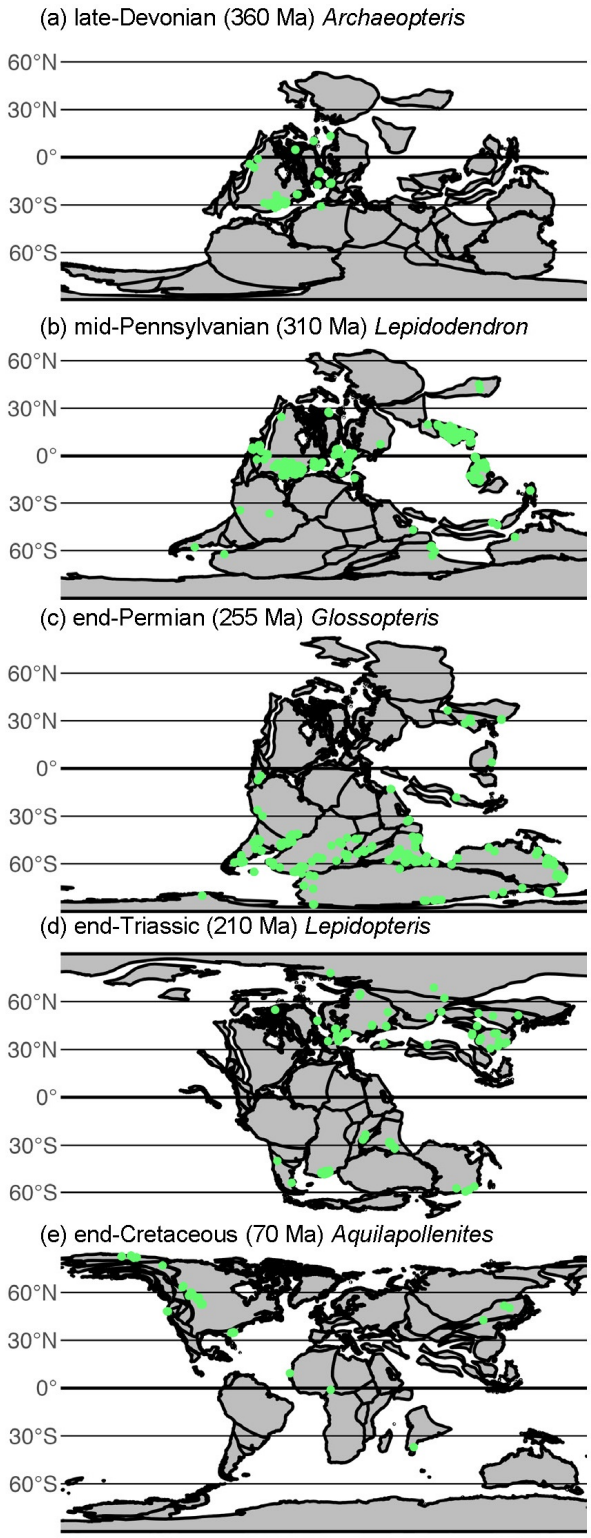


Figure 1

Geographic ranges of common taxa that went extinct or were extirpated from most regions during past mass extinction and/or ecosystem collapse events. Occurrence data for: **a** fossil-genus *Archaeopteris* (and associated taxa), a large-stature, spore-bearing tree in the Late Devonian; **b** fossil-genus *Lepidodendron* (and associated taxa), a large swamp-dwelling tree in the Mid-Late Pennsylvanian Boundary; **c** fossil-genus *Glossopteris* (and associated taxa), a woody tree in the end-Permian; **d** fossil-

genus *Lepidopteris* (and associated taxa), a possible woody vine, in the end-Triassic; and **e** fossil-genus *Aquilapollenites* (and associated taxa), the pollen of a possible hemiparasitic plant in the end-Cretaceous. Ecosystems or floral provinces (a to e) are typified by the genera listed on the maps (full list of occurrence taxa in Supporting Table 1).

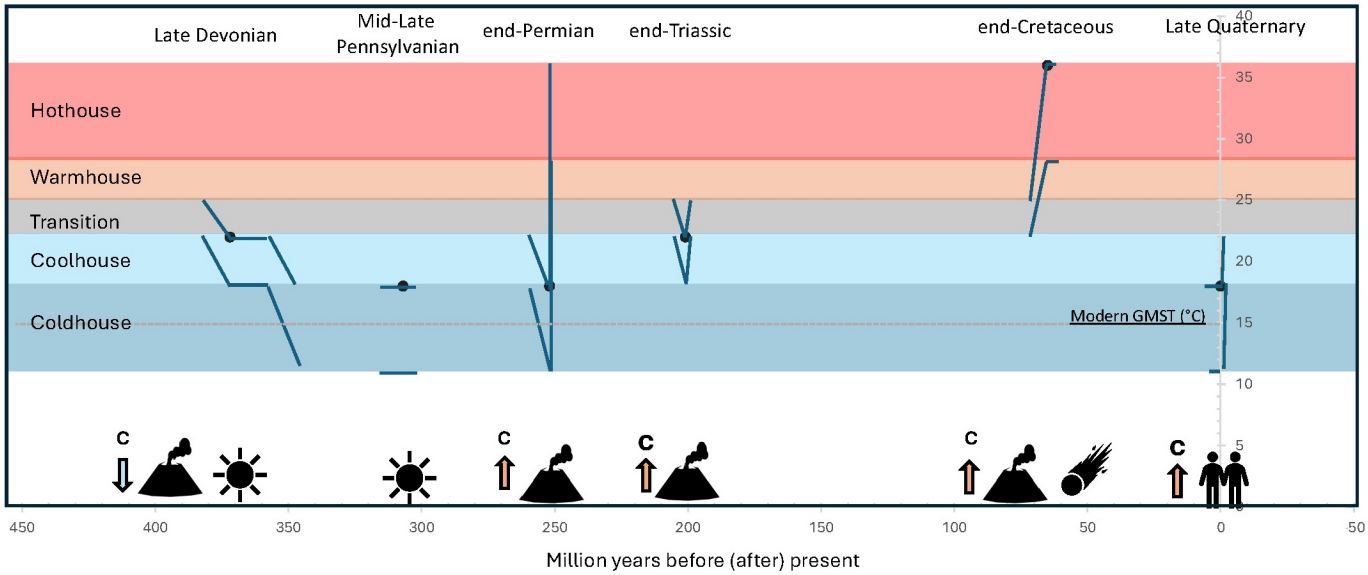


Figure 2

Long-term climatic context for Earth's mass extinction events. Climate state analysis from[32]. The chart plots the climate state [coldhouse (11 to 18°C), coolhouse (18 to 22°C), transition (22 to 25°C), warmhouse (25 to 28°C), hothouse (28 to 36°C)] of the geological stage preceding and following four of the 'big 5' mass extinction events, in addition to the Mid-Late Pennsylvanian boundary episode and contemporary (late Quaternary) extinctions. Icons indicate the primary extinction drivers for each event and whether they were carbon-sink (down arrow) or carbon-source (up arrows) events[31,186,187]. The timeline of late Quaternary climate state change is plotted from Pliocene to present and projected forward 1.5 million years to provide a million-year timescale comparison with deep-time events. Current global mean surface temperature is 15°C and classified as a coolhouse climate state[32]. Conservatively, it is assumed that Earth will transition from coldhouse to coolhouse within the next century and will exceed 608 ppm atmospheric CO_2. This comparative framework shows that all faunal mass extinction events considered in this paper (Late Devonian, end-Permian, end-Triassic, end-Cretaceous) occurred within a backdrop of climate state change, but the Mid-Late Pennsylvanian episode did not. The analysis also suggests that no mass extinction is the perfect analogue for our current extinction interval, with different primary (ultimate) drivers, starting from different climate states and/or undergoing different magnitudes and/or signs of climate state changes. Two mass extinction events occurred against a backdrop of warmhouse and hothouse climate states – the end-Permian and end-Cretaceous. Two mass

extinction events occurred within a single climate state – Mid-Late Pennsylvanian and late Quaternary – both with superimposed Milankovitch scale climate perturbations[63]. Two occurred against the backdrop of three climate state changes – the Late Devonian and end-Permian. GMST = global mean surface temperature.

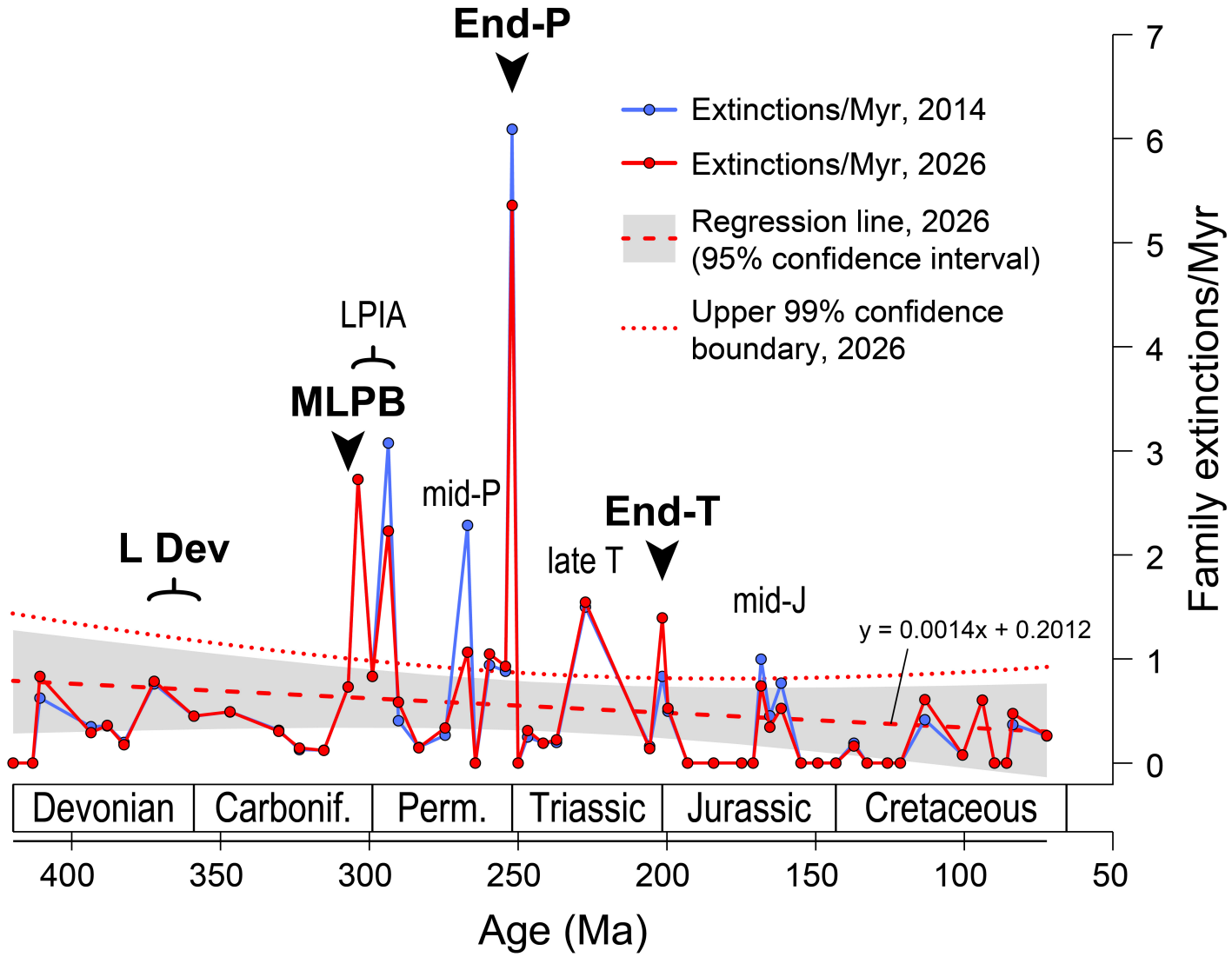


Figure 3

Extinction rates for vascular plant (tracheophyte) families from the Devonian to Cretaceous. Raw data are from[2]. The original data (labelled '2014') have been plotted alongside the reanalysed dataset (labelled '2026'), which incorporates the latest chronostratigraphic stage durations[177]. All events with extinction rates above the upper 95% confidence interval are considered plant mass extinctions, following the criterion for marine invertebrates by Raup & Sepkoski[1] (Extended Table 1). Those intervals in bold are discussed further in this paper. Note that the extinction rate of the mid-late Pennsylvanian boundary (MLPB) precedes the two Late Paleozoic Ice Age (LPIA) peaks. Abbreviations: L Dev = late

Devonian; mid-P = mid-Permian (Roadian and Capitanian stages); Late T = Late Triassic (Carnian Stage); End-T = end-Triassic; mid-J = mid-Jurassic; End-P = end-Permian.

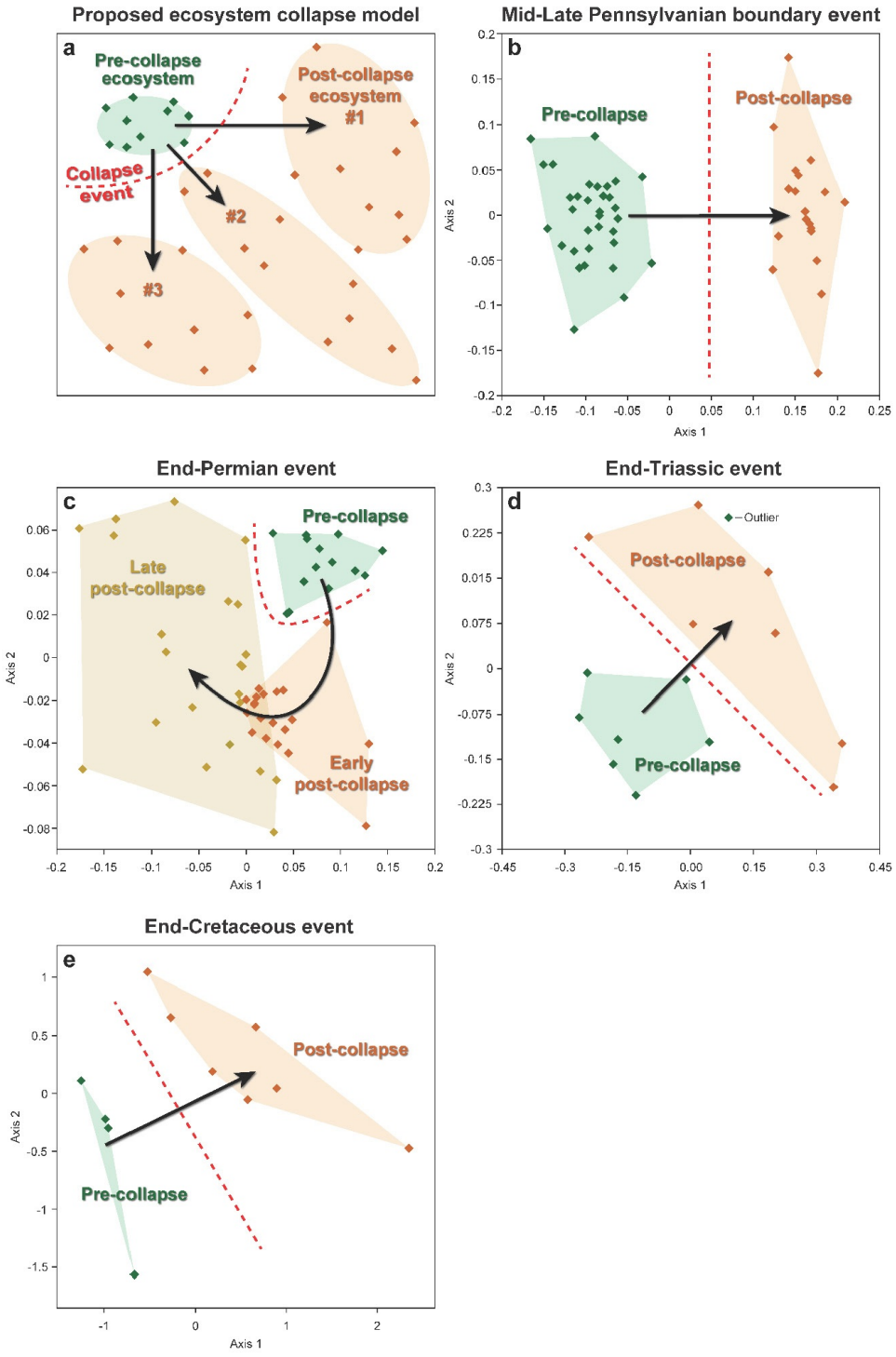


Figure 4

Ecosystem collapse events represented by non-metric multidimensional scaling (NMDS) ecospaces. Each point is a dataset of fossil plant abundances, and represents one ecosystem state in either the pre-

event (green shaded sector) or post-event (orange-shaded sector) ecosystems. **a** New collapse model proposed here, based on deep-time collapse events (b–e). Firstly, the prehistoric records clearly support hypothesis 1 (and reject hypothesis 2) of the IUCN collapse model (Extended Table 1). Secondly, owing to the long timescales that the fossil records provide, they can illustrate the long-term natural variations in ecosystem compositions (represented by ecospace area size). The post-collapse ecosystems typically have larger ecospace areas than those of the pre-collapse intervals, indicative of major, long-term ecosystem instability. Lastly, no recurrent, specific directions of ecosystem shift following collapse (i.e., post-collapse ecosystem #1, #2 or #3) have yet been observed, but the fossil record offers a unique, empirical approach to test this. **b** Mid-Late Pennsylvanian Boundary (MLPB) event based on spore-pollen data of Illinois Basin, USA[183]. Note: the ordination areas are similar, but this may be because the pre-event Desmoinesian Stage is substantially longer than the post-event Missourian Stage[188]. **c** End-Permian event based on spore-pollen data of eastern Australia[110]. Note 1: Despite representing a relatively short stratigraphic interval (c. 95 m vs c. 23 m in stratigraphic thicknesses), the early post-collapse ecospace is larger than that for the pre-collapse interval. Note 2: The late post-EPE sector—which extends for several million years following the collapse—indicates a permanent ecospace shift. **d** End-Triassic event based on macrofossil data from two localities of east Greenland[24,25]. Note: the outlier sample (bed 3 Astartekløft), which might represent a transitional change from pre- to post-event assemblages. **e** End-Cretaceous event based on macrofossil data, northwestern USA[158].

Supplementary Files

This is a list of supplementary files associated with this preprint. Click to download.

- McElwainetalExtendedDataNEE0426.docx
- SupportingTable1McElwainetal.xlsx
- SupportingTable2McElwainetal1.xlsx
- SupportingTable3McElwainetal.xlsx